MJSAT

Malaysian Journal of Science and Advanced Technology

journal homepage: https://mjsat.com.my/

The Study of MPPT Algorithm for Solar Battery Charging System

Heh Chee Yang*[1], Jabbar Al-Fattah Yahaya[1], and Asmarashid Ponniran[1]

[1] *Dept. of Electrical Engineering, Faculty of Electrical and Electronic Engineering, Universiti Tun Hussein Onn Malaysia. Batu Pahat, Malaysia.*

KEYWORDS

MPPT
Solar Energy
Battery Charging
PV Panel
MATLAB

ARTICLE HISTORY

Received 9 July 2022
Received in revised form 14 July 2022
Accepted 7 August 2022
Available online 14 August 2022

ABSTRACT

Renewable energy is a topic that is frequently researched recently due to the negative environmental changes brought by using non-renewable energy sources such as fossil fuels. The application of the renewable energy is wide including being used to charge a battery using buck converter in general charging system. However, the problems faced by these solar charging systems is the inability to regulate and stabilize the output of the PV module, causing the loss of efficiency of PV module. A mechanism that is used to solve the problem is to develop the algorithm for maximum power point tracking in PV module. Thus, the project aims to improve the performance of battery charging system by using different MPPT algorithms and compared their performance with issues being analyzed, and helped to suggest the best algorithm to maximize the power supply and consumption effectively based on the MATLAB/Simulink results. The MPPT techniques used in the study consist of Constant Voltage (CV), Perturb and Observe (P&O), Incremental Conductance (INC) and also Hill Climbing (HC). The algorithms will be used on buck converter and compared with conventional solar battery chargers that uses PID controller for voltage regulation. The results are obtained from measurements of various parameters and they will be compared with the theoretical value with error calculation to determine the efficiency of the mechanism and also analyzed to determine the causes and effects of the simulation and for comparison. The results show that different algorithms can affect the performance of the system, such as changing transient times, power efficiency, shape of graph and so on. In conclusion, the best algorithm is Incremental Conductance due to its high-power efficiency and stable parameter output for battery charging system, in which further work done can be continued to include more weather data and constructing complex algorithm as well.

1. INTRODUCTION

Renewable energy is currently a frequently researched topic by scientists around the world in order to tackle the issues caused by recent changes in terms of environmental conditions and electricity demand. Due to frequent usage of non-renewable energy sources such as natural gases and fossil fuels, the earth is currently facing the crisis of climate change that affects the livelihood of many people. The search for a more sustainable alternative energy becomes very urgent and critical to ensure the sustainability of the environment. Thankfully, several renewable alternative energy sources have been researched and experimented with very promising results, one of them being solar energy. Currently, a lot of electrical and electronic industry are gradually transitioning from using traditional electrical source to a cheaper and infinitely sourced renewable energy with emphasis on renewable energy storage using battery component as well. Batteries is a kind of energy storage components with a wide variety of applications, such as in telecommunications, electric vehicles, and uninterruptible power supply. The design of the battery charging system affects the sustainability of the battery such as its battery life and charging capacity. Using conventional charging design involving AC-DC converter can easily result in power dissipation and reducing the efficiency

*Corresponding author:
E-mail address: Heh Chee Yang < uthmhcy7@gmail.com >.

of battery charging system, thus in this report a DC-DC converter solar power battery charger is proposed using buck converter for both conventional solar battery charger and MPPT solar battery charger, with a voltage regulator used in their respective systems in order to control the output voltage. The buck converter is a basic topology of the DC-DC converter that converts the high DC input voltage to a low DC output voltage. Its high efficiency and simplicity in design makes the converter to be commonly used in various power electronic applications, according to Sujedto (2018) and others [1].

For the voltage regulator, it has also another name called charge controller, where it is connected between the input voltage (PV cells) and output voltage (battery). The purpose of the component is to regulate the voltage by using feedback loop to ensure the battery is charged properly without overvoltage or undervoltage condition to maximize the battery life. For the conventional battery charger design, a pulse width modulation controller (PWM) is used to regulate the voltage, while MPPT battery charger design uses maximum power point tracking controller (MPPT). Among the techniques of MPPT are incremental conductance (IC) and perturb & observe (P&O) according to Lapsongphon and Nualyai (2021) [2]. This report will compare the design and performance of conventional solar battery charger and MPPT solar battery charger using the general design of battery charging system and simulate in MATLAB/Simulink software application and choose the best design in terms of performance and efficiency. Figure 1 shows a solar buck converter battery charging system.

Fig. 1. Example of Solar Buck Converter battery charger.

One major problem of the PV system source supply is the instability of the output current or voltage from its system due to various issues such as frequent changes of inner and outer condition. For the PV system to supply electricity voltage, it must absorb light energy from the sun which is also known as irradiance and convert the light energy into electrical energy for the circuit to run. Without using any medium that stabilizes the output voltage or current, the power flow in the system can become easily out of control due to the supply voltage is directly proportional to the irradiance and the surrounding temperature. Thus, any major changes in the irradiance and surrounding temperature, such as weather changes from sunny day to rainy day, will affect the efficiency of the battery charging system. This situation is even worse for a battery load even under fixed temperature and irradiance due to its charging mechanism that makes it an active load that makes its current and voltage inconsistent. Thus, it is strongly recommended to install a mechanism that stabilizes and controls the flow of electricity power in the system, such as using voltage controller and buck converter instead of directly connecting the PV system to the battery load directly. However, even conventional charging system that only utilizes buck converter and voltage controller does not solve the optimization problem in a battery charging system effectively. This is because other factors involving the PV array such as I-V characteristics and power losses are not considered, thus ended up having a less effective power usage of solar PV array, even under stable weather conditions. The buck converter itself can be imagined as equivalent to variable resistor, where its resistance will either increase or decrease the output of the voltage. However, without regulation, the electrical power in the circuit that is meant to be used by the battery at the load become loss through heat dissipation due to unregulated I-V characteristics, where only voltage parameter is adjusted while the current parameter is ignored, thus resulting in power usage not maximized. So even though the output voltage is controlled and stabilized, the I-V characteristic of the PV array causes the power consumption of the solar battery charger to be less optimized.

PV array system is a very complex power source circuit. With addition of the battery load which has nonlinear output characteristics that frequently changes based on I-V characteristics and state-of-charge makes it a challenging task to control the power flow of the battery charging system. Having an algorithm that tracks the changes within the circuit itself in addition to atmospheric condition such as irradiance and temperature condition and making suitable adjustments to track for the maximum power point is important for the system to run efficiently and last longer, as noted by Podder and others (2019) [3]. At the very least, the power efficiency of the system should be optimal even under stable weather condition. Thus, issues such as voltage variation, ripples and oscillations, as well as power losses are required to be analyzed and determined which MPPT handles these issues the best.

It is hypothesized that the performance of the battery charger is better with MPPT algorithm being used instead of conventional design due to its maximum power point tracking mechanism. The aim is to understand how the MPPT algorithm works with the solar battery charger system and how does the algorithm improve upon conventional design system for the circuit using maximum power point tracking mechanism. This research work embarks on the following objectives: to improve the performance of battery charging system using MPPT algorithm, to compare the difference between the performance of the conventional solar battery charging system with MPPT-based solar battery charging system to analyze and overcome the performance issues, and to determine the best MPPT algorithm for the solar battery charging system. For the scopes of the research, the battery parameter is limited to using the same voltage of battery for all the battery charging systems for consistency. The DC-DC converter used in the conventional and MPPT-based design will only focus on buck converter. Single solar cell with 210W power is used for the PV source supply for all designs with fixed irradiance and temperature being used. The controller design is limited to using PID controller for the conventional design and 4 types of MPPT algorithm for MPPT-based design. Parameters to analyze the performance of circuits are limited to voltage, current, oscillation, power performance as well as changes of state-of-charge. This project will help to provide clear understanding on the steps to develop a general

solar battery charging system, ideas on how to utilize MPPT algorithm for any type of general solar battery charging system and a clearer comparison on the difference in performance of MPPT and non-MPPT battery charger circuit design. In this project report, a conventional solar battery charger and a few MPPT solar battery chargers are designed and simulated in MATLAB Simulink. Through this experiment, it is expected that we can obtain the measurements of the output and input parameters such as voltage and current and compared with each other to find out the efficiency of the system. The designs are expected to be functioning for the battery charger to run and charge the lead-acid battery, as indicated by the state-of-charge of the battery slowly increasing over a period charging the circuit. The report will also provide details on designing a general battery charging system with other components such as PV, buck converter, battery, and voltage controller as well as MPPT algorithm for MPPT-based solar charging system.

2. METHODOLOGY

2.1 Block Diagram

For the methodology, the conventional solar battery charger is designed based on the recommended ratings in the PV module, DC-DC buck converter, voltage controller and battery size. In MPPT solar battery charger, the MPPT algorithm will replace the voltage controller from the conventional solar battery charger design. Figure 2 shows the general block diagram design for conventional battery solar charger system while Figure 3 shows the block diagram design for MPPT solar battery charger system using 3 MPPT algorithms which are CV, P&O, INC and HC as well. Generally, the changes in block diagram are the mechanism of recalibrating the parameters for maximizing output performance, in which the details of each components' specification will be provided in this section for methodology research purpose. The conventional solar battery charger is closed-loop while the MPPT solar battery charger is in open-loop.

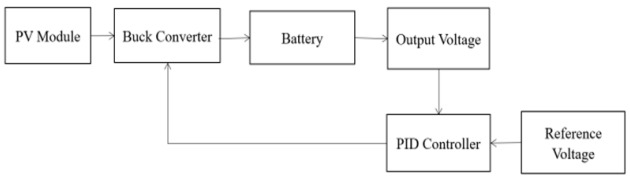

Fig. 2. Block Diagram of Conventional Solar Battery Charger

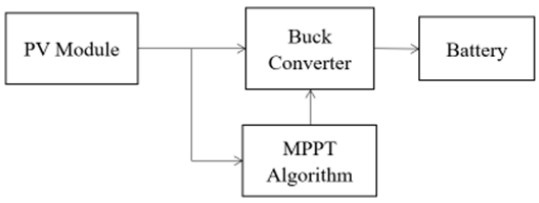

Fig. 3. Block diagram of MPPT Solar Battery Charger,

2.2 Materials and Methods

a) *PV Module*: For the PV module, the rated power of 210W for a single PV module is chosen. The buck regulator of solar power charger is planned to have an input voltage of range about 28 V ~ 36 V and rated power of 210W. An RC low pass filter with resistance of 0.0001 Ohms and capacitance of 0.001 Farad is installed at the output side of PV module in order to stabilize the voltage and current of the system. A bus selector and unit delay blocks with displays are connected to the measurement port of the PV module in order to record the output values of the PV module such as current, voltage and power. Table 1 gives the specification of other parameters of the PV module.

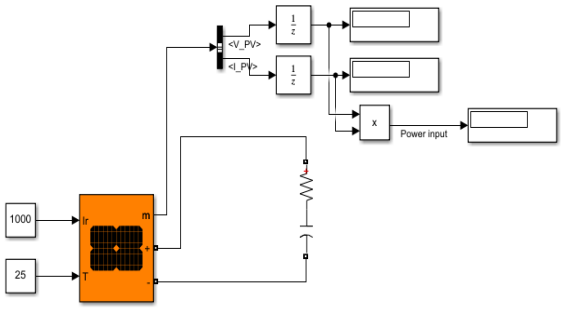

Fig. 4. Circuit design of PV module with current and voltage sensors

Table 1. Parameter specification of PV module

Parameters	Value
Maximum Power (W)	213.15
Cells per module	60
Open circuit voltage, V_{OC} (V)	36.3
Short-circuit current, I_{SC} (A)	7.84
Temperature (°C)	25
Irradiance (W/m^2)	1000

b) *Output Load*: For the output load, it consists of a battery and a diode. For the battery, which is the main output load, a 15V lead-acid type single battery is designed at the output side of the buck converter. Lead-acid type battery is chosen due to its large depth of discharge and also bigger autonomous control which is suitable for PV system as postulated by Rezzak and others (2018). [4] The parameters are assumed to be nominal, however during simulation, there will be deviation since the battery changes its own voltage and current as it is charged by the solar power. The nominal output voltage is set as 15 V, and the rated capacity is at 100 Ah, and the state of charge is set at 30% with a response time of 1s because that is the point where maximum power of 210 W can be nearly reached. The discharge rate is determined by the nominal parameters of the battery. For the diode, it is used to stabilize the output parameters with a minimum resistance parameter provided in Table 2 that barely affects the outcome of the battery parameters. The negative gains connecting to

output displayer reverses the polarity of the values shown, so that the power output and current output are positive values. They are negative due to the battery itself being an active component.

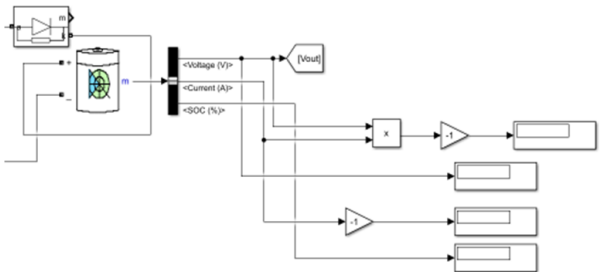

Fig. 5. Circuit design of lead acid battery with diode, current and voltage sensors.

Table 2. Parameter Specification of PV Module

Parameters	Value
Resistance, R_{ON} (Ω)	0.001
Inductance, L_{ON} (H)	0
Forward voltage, V_f (V)	0.8
Snubber resistance, R_S (Ω)	500
Snubber capacitance, C_S (F)	250×10^{-9}

c) *DC-DC Buck Converter*: For the DC-DC buck converter, the output voltage at the battery is given Vo = 15 V and the percentage of voltage ripple and current ripple is assumed to be at 1% and 10% respectively. The switching frequency, f_{SW} is chosen to be at 25 kHz so that acoustic noise can be negligible, but not too high so that values of inductor and capacitor do not go too low and causing power loss. An ammeter is installed near the inductor to obtain the inductor value, and the diode and MOSFET uses default parameters. The circuit design and parameter specification are provided below, while the calculation details of the converter will be provided in Section 2.3 (Equations) later.

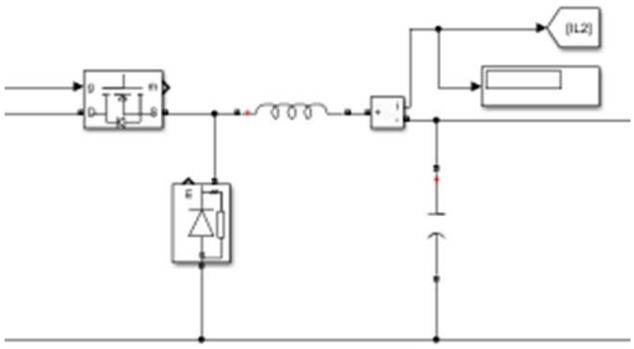

Fig. 6. Circuit design of DC-DC Buck Converter.

Table 3. Parameter Specification of MOSFET

Parameters	Value
FET resistance, R_{ON} (Ω)	0.1
Internal diode inductance, L_{ON} (H)	0
Internal diode resistance, R_d (Ω)	0.01
Internal diode forward voltage, V_f (V)	0
Snubber resistance, R_S (Ω)	1×10^{5}
Snubber capacitance, C_S (F)	∞

Table 4. Parameter Specification of Diode

Parameters	Value
Resistance, R_{ON} (Ω)	0.001
Inductance, L_{ON} (H)	0
Forward voltage, V_f (V)	0.6
Snubber resistance, R_S (Ω)	500
Snubber capacitance, C_S (F)	250×10^{-9}

d) *Voltage Controller*: This design only applies for conventional solar battery charger. For voltage controller, a close loop system is constructed with PID control, where the difference of reference value for output voltage and the real output voltage from real-time simulation is taken and converted in PID controller. There are many methods to find out the parameter of Kp, Ki and Kd. Here, a simple trial and error method is used where Ki and Kd are set to zero initially. The Kp is gradually increased by 10% until the output oscillates, then the Kp is decreased until oscillation is eliminated. Next, Ki is set by a fraction of Kp to correct the offset in the duration. Kd is normally not required unless the values is required to quickly stabilize to reference value after initial oscillation. The values are Kp=0.84, Ki=0.48, and Kd=0.01. The values are then converted to duty ratio as output for PWM which will transfer to gate of MOSFET. The repeating sequence is also generated to match the switching frequency as well.

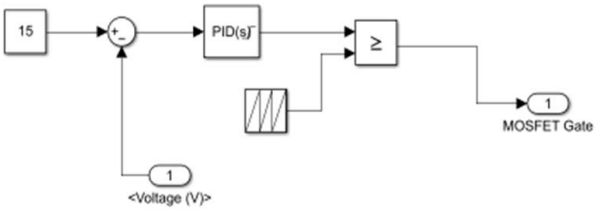

Fig. 7. Circuit design of Voltage Controller.

e) *MPPT Algorithms*: This design only applies for MPPT solar battery charger. Here the design is the modification of voltage controller by replacing the PID controller with a function block consisting of MPPT coding. The inputs of these algorithms are taken from the PV module voltage and current directly. The coding of the algorithm is based on the flowchart of the algorithms from various references as seen below. The repeating sequence component is set to 25 kHz as switching frequency. The MPPT algorithms being used are Perturb & Observe (P&O), Incremental Conductance (INC), Constant Voltage (CV) and Hill Climbing (HC).

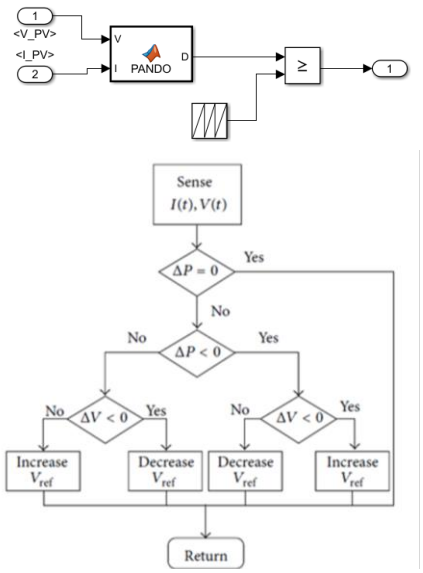

Fig. 8. Circuit design and simplified flowchart of P&O [5].

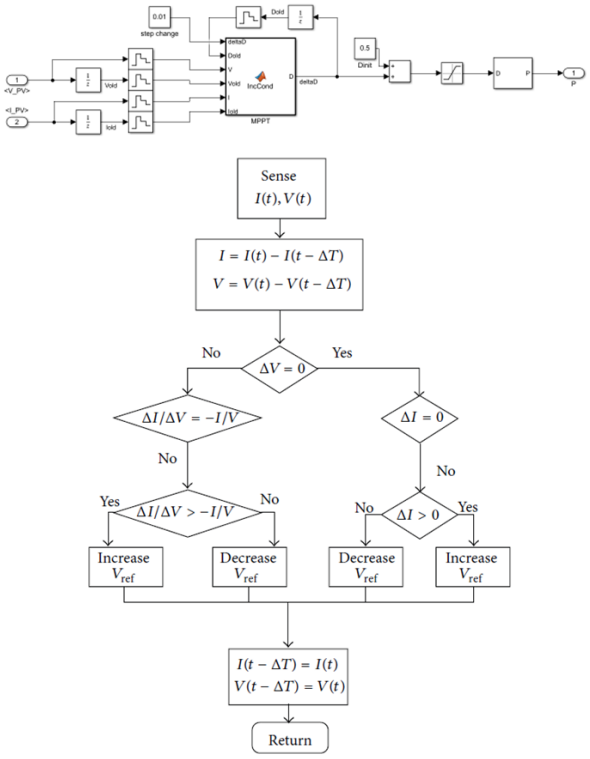

Fig. 9. Circuit design and simplified flowchart of INC [5].

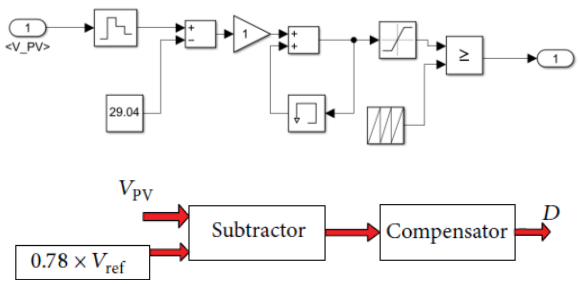

Fig. 10. Circuit design and simplified flowchart of CV [5].

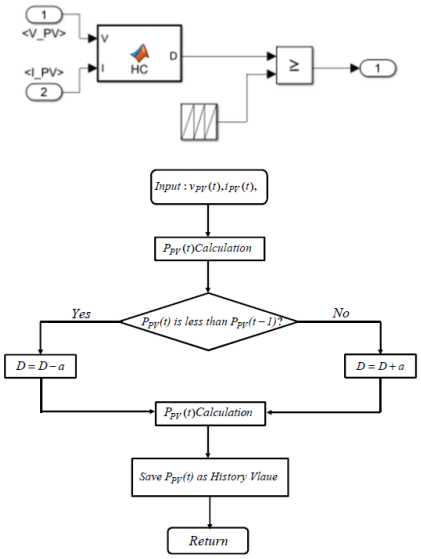

Fig. 11. Circuit design and simplified flowchart of HC [6].

2.3 Equations

For the calculation of the buck converter specifications, based on the values provided for DC-DC buck converter. We first calculate the duty ratio, which is given as:

$$D = \frac{V_o}{V_i} = \frac{15V}{28V} = 0.5357 \quad (1)$$

The input voltage is taken from the smallest value (28V), since the input voltage changes around that range. The device chosen is MOSFET. For input, the calculation of voltage and current is:

$$I_i = \frac{P_i}{V_i} = \frac{210W}{28V} = 7.5A \quad (2)$$

Again, input voltage is taken at smallest value. In real-time simulation, the solar input ranges between 28 V and 36 V. The output nominal resistance and current is calculated as below:

$$I_o = \frac{P_o}{V_o} = \frac{210W}{15V} = 14A \quad (3)$$

$$R = \frac{V_o}{I_o} = \frac{15V}{14A} = 1.0714\Omega \quad (4)$$

Since the resistance of the battery is dynamic due to constant changing of the voltage and current during charging, the optimal calculation of L and C is based on the voltage ripple and current ripple. The calculation of voltage ripple, current ripple, inductance, capacitance and minimum inductance is based on the buck converter formulas:

$$\Delta I_o = 10\% I_o = 10\% \times 14A = 1.4A \quad (5)$$

$$\Delta V_o = 1\% V_o = 1\% \times 15V = 0.15V \quad (6)$$

$$L = \frac{V_o(V_i - V_o)}{\Delta I_o \times f_{sw} \times V_i} = \frac{15V(28V - 15V)}{1.4A \times 25000Hz \times 28V} = 0.199mH \quad (7)$$

$$C = \frac{\Delta I_o}{8 \times \Delta V_o \times f_{sw}} = \frac{1.4A}{8 \times 0.15V \times 25000Hz} = 46.667\mu F \quad (8)$$

$$L_{min} = \frac{(1-D)}{2f_{sw}} R = \frac{(1-0.5357)}{2 \times 25000Hz} \times 1.0714\Omega = 9.949\mu H \quad (9)$$

By comparing L_{min} with previously calculated inductance (L) using ripple method, we can see that inductance (L) is larger than L_{min}. Thus, the circuit will operate in continuous conduction mode (CCM).

$$r = \frac{\Delta V_o}{V_o} = \frac{0.15V}{15V} = 0.01 \quad (10)$$

$$C_{min} = \frac{(1-D)}{8L_{min}rf_{sw}^2} = \frac{(1-0.5357)}{8 \times (9.949 \times 10^{-6})H \times 0.01 \times (25000Hz)^2} = 933\mu F \quad (11)$$

We can see that C_{min} is larger than the proposed capacitance (C) value. These values are the minimum requirement for the circuit to be operated barely at continuous conduction mode. A full continuous mode needs the inductance value to be around 10 times larger than L_{min}, and the proposed value of inductance (L) exceeded 10 times, hence the buck solar charger will operate in continuous conduction mode.

3. Results and Discussions

This section will discuss and analyze about the conventional solar battery charger system performance as well as the MPPT solar battery charger system for P&O, INC, CV and HC algorithms. The system performance is analyzed based on their deviation with voltage, current and power from the expected results computed using theoretical formula. Comparisons are also made in between the graph output and value output with power efficiency calculation and other parameters to find out the best MPPT algorithm that can be used.

3.1 Conventional Solar Battery Charger

The overall conventional solar battery charger circuit diagram is constructed. The component POWERGUI is set up with discrete time of 1μs to run the simulation. The simulation is run and the result is recorded and shown at Table 5. In theory, BUCK convertor will show that the output values is lower than the input values and the simulated results shown the same. In the beginning, the input voltage is set from 28 to 36V and the output values is 14.5V. In Figure 12, the graph of V_{in} is observed to be decreasing at a steady rate. For V_o graph, the battery is charging with the voltage increasing at a steady rate instead. At 28 V of input, the inductor current is sawtooth shape without reaching 0 A, hence the buck converter operates in continuous conduction mode. The output current also takes a longer time to reach steady state due to optimization issues in using PID controller.

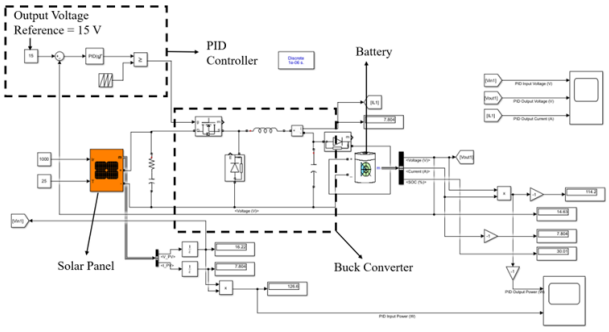

Fig. 12. Circuit design of conventional solar battery charger.

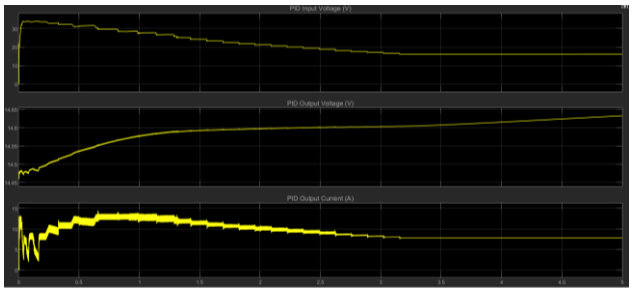

Fig. 13. (From Top to Bottom) Input voltage, output voltage and output current.

For P_o graph, we can observe that the graph shape is similar to output current I_o which also takes a long time to reach steady state, hence we can infer that the output power is mostly influenced by the output current with its irregular current changes before reaching steady state which takes a long time, with the output voltage only having minor influence with a small rate of increase in its voltage. The power ripple is also more noticeable in output power compared to input power P_I due to the capacitor and inductor components influencing the output power. This shows that PID controller is not suitable for optimization when the system uses non-linear load such as battery which dynamically changes as noted by Ardhenta and others (2020). [7]

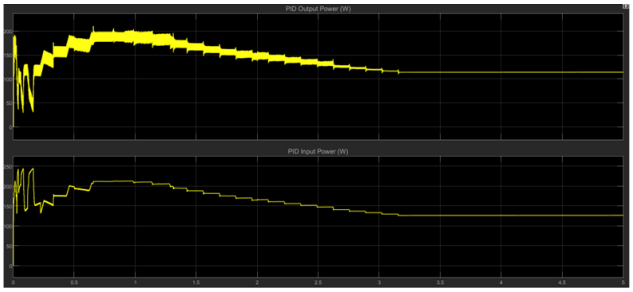

Fig. 14. (From Top to Bottom) Output power and input power.

The graphs are obtained from the scopes connected to inputting parameters with simulation time set at 5 seconds. The expected results are obtained from the parameters in Methodology section, and the simulation results are obtained from the display outputs in MATLAB at 5 seconds. The percentage error is calculated based on the formula below:

$$\%\ Error = \frac{|Simulation\ Results| - |Expected\ Results|}{|Expected\ Results|} \times 100\% \quad (12)$$

The error values can be obtained by comparing the value calculated and the value recorded. The state of charge error is ignored for the comparison because the battery's state of charge is expected to increase due to the charging operation. The output power parameter gives the highest amount of error output, while the output voltage has the smallest amount of error output. The errors happen due to resistances in components as well as imperfect parameter specification for PID and capacitors and inductors, as well as power losses in the system happens. According to Faraday's law of induction, there will be a voltage V_L induced across the inductor where it opposes the flow of input voltage. This causes the reduction of output voltage at the battery and thus impacting the overall performance. At the same time, the inductor absorbs energy

from the source and stores the energy in the form of a magnetic field.

Table 5. Simulation Result of Conventional Solar Battery Charger

Parameters	Simulation Results	Expected Results	% Error
Input Power, P_I (W)	126.6	213.15	-40.61
Input Voltage, V_I (V)	16.22	28	-42.07
Input Current, I_I (A)	7.804	7.5	4.05
Output Voltage, V_O (V)	14.63	15	-2.47
Output Current, I_O (A)	7.804	14	-44.26
State of charge (%)	30.01	30	0.03
Output Power, P_O (W)	114.2	210	-45.62

3.2 Perturb & Observe (P&O) Solar Battery Charger

The overall P&O solar battery charger circuit diagram is constructed as shown in Figure 14. The component POWERGUI is set up with discrete time of 1μs to run the simulation. The simulation is run and the result is recorded and shown at Table 6. In Figure 16, we can see that the graph of input voltage reaches a steady state with an average of 30V. The voltage ripple is very noticeable in the graph. For Vo graph, the battery is charging with the voltage slowly increasing at a constant rate with a more noticeable voltage ripple as well. At 28 V of input, the inductor current is reaching 0 A, hence the buck converter operates in discontinuous conduction mode.

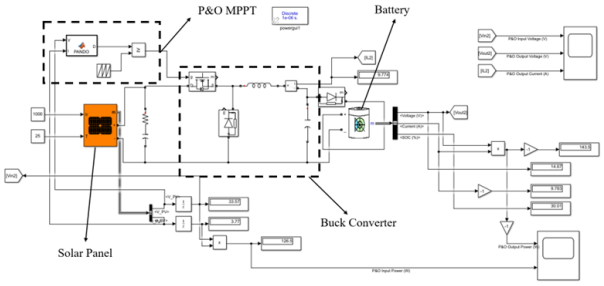

Fig. 15. Circuit design of Perturb & Observe solar battery charger.

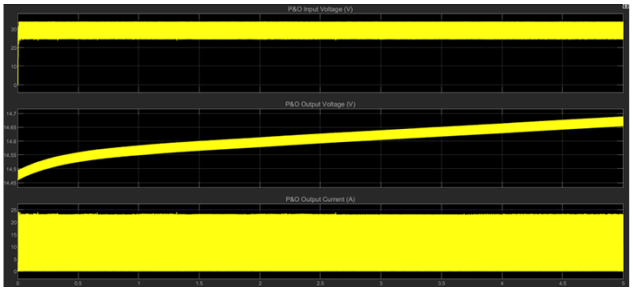

Fig. 16. (From Top to Bottom) Input voltage, output voltage and output current.

For P_o graph in Figure 16, we can observe that the graph shape is similar to output current I_o which also reaches 0 W due to the shape of graph of output current with the output voltage only having minor influence with a small rate of increase in its voltage. The output power is unusually having a higher power than input power due to the power being distributed into triangle waveform instead of square waveform. Due to the formula of power being the product of voltage and current, a normal power output graph will be in square waveform, but since the current is in discontinuous current mode with its waveform being triangle shape, the output power also changes accordingly. The power ripple is also more noticeable and unstable in input power when compared with other circuits with different MPPT algorithms.

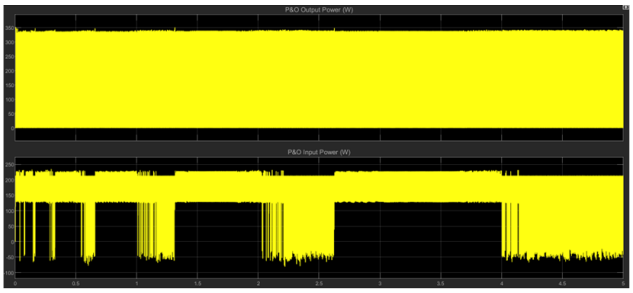

Fig. 16. (From Top to Bottom) Output power and input power.

The error values can be obtained by comparing the value calculated and the value recorded. The input current parameter gives the highest amount of error output, while the output voltage has the smallest amount of error output. The errors happen due to resistances in components as well as imperfect parameter specification for capacitors and inductors, as well as power losses in the system happens. According to Faraday's law of induction, there will be a voltage V_L induced across the inductor where it opposes the flow of input voltage. This causes the reduction of output voltage at the battery and thus impacting the overall performance. At the same time, the inductor absorbs energy from the source and stores the energy in the form of a magnetic field.

Table 6. Simulation Result of P&O Solar Battery Charger

Parameters	Simulation Results	Expected Results	% Error
Input Power, P_I (W)	126.5	213.15	-40.65
Input Voltage, V_I (V)	33.57	28	-19.89
Input Current, I_I (A)	3.77	7.5	-49.73
Output Voltage, V_O (V)	14.67	15	-2.2
Output Current, I_O (A)	9.783	14	-30.12
State of charge (%)	30.01	30	0.03
Output Power, P_O (W)	143.5	210	-31.67

3.3 Incremental Conductance (INC) Solar Battery Charger

The overall INC solar battery charger circuit diagram is constructed as shown in Figure 17. The component POWERGUI is set up with discrete time of 1μs to run the simulation. The simulation is run, and the result is recorded and shown at Table 7. In Figure 18, we can see that the graph of input voltage reaches a steady state with an average of 30V, but the stability of input voltage is slightly lower. For V_o graph, the battery is charging with the voltage slowly increasing at a constant rate with a tiny amount of voltage ripple being observed as well. For the inductor current, the transient time is slightly slower than other MPPT with fast transient time, but the steady state of the inductor current has occasional spikes in certain times as well as having a more noticeable current ripple in the graph.

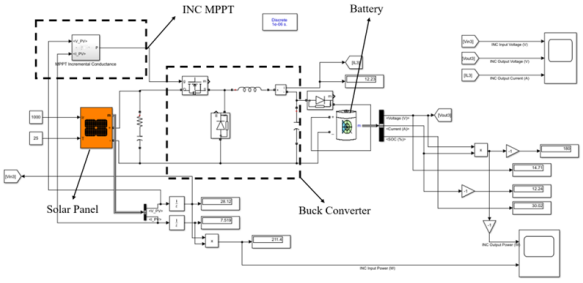

Fig. 17. Circuit design of incremental conductance solar battery charger.

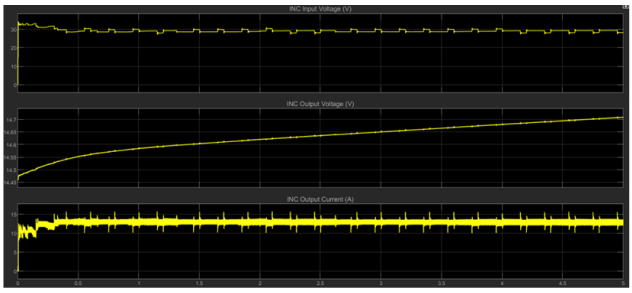

Fig. 18. (From Top to Bottom) Input voltage, output voltage and output current.

For P_o graph, we can again observe that the graph shape is similar to output current I_o, hence we can infer that the output power is mostly influenced by the output current with its irregular current changes before reaching steady state, with the output voltage only having minor influence with a small rate of increase in its voltage. The power ripple is also more noticeable in output power compared to input power P_I due to the capacitor and inductor components influencing the output power.

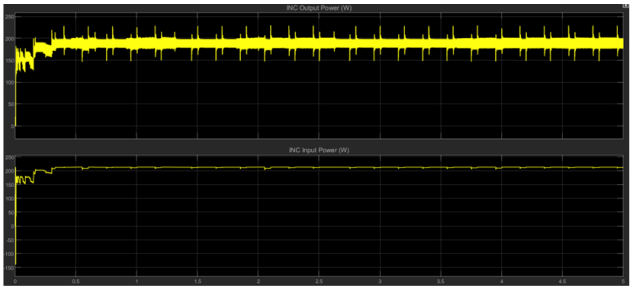

Fig. 19. (From Top to Bottom) Output power and input power.

The error values can be obtained by comparing the value calculated and the value recorded in Table 7. The output power parameter gives the highest amount of error output, while the input current has the smallest amount of error output. The errors happen due to resistances in components as well as imperfect parameter specification for capacitors and inductors, as well as power losses in the system happens. According to Faraday's law of induction, there will be a voltage V_L induced across the inductor where it opposes the flow of input voltage. This causes the reduction of output voltage at the battery and thus impacting the overall performance. At the same time, the inductor absorbs energy from the source and stores the energy in the form of a magnetic field.

Table 7. Simulation Result of INC Solar Battery Charger

Parameters	Simulation Results	Expected Results	% Error
Input Power, P_I (W)	211.4	213.15	-0.82
Input Voltage, V_I (V)	28.12	28	0.43
Input Current, I_I (A)	7.519	7.5	0.25
Output Voltage, V_O (V)	14.71	15	-1.93
Output Current, I_O (A)	12.24	14	-12.57
State of charge (%)	30.02	30	0.07
Output Power, P_O (W)	180	210	-14.29

3.4 Constant Voltage (CV) Solar Battery Charger

The overall CV solar battery charger circuit diagram is constructed as shown in Figure 20. The component POWERGUI is set up with discrete time of 1μs to run the simulation. The simulation is run and the result is recorded and shown at Table 8. In Figure 21, we can see that the graph of input voltage reaches a steady state with an average of 30V with a very stable and constant output with little voltage ripple. For V_o graph, the battery is charging with the voltage slowly increasing at a constant rate with a tiny amount of voltage ripple being observed as well. For the inductor current, the steady state of the inductor current has a more noticeable current ripple in the graph. The graphs also show a faster transient time for the graph to be at a steady state.

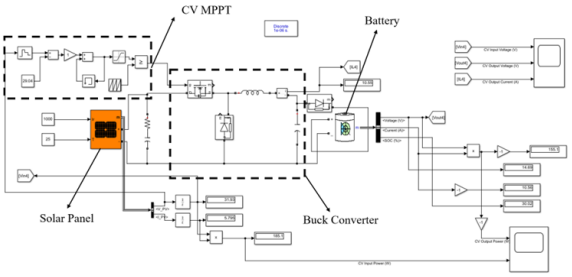

Fig. 20. Circuit design of constant voltage solar battery charger.

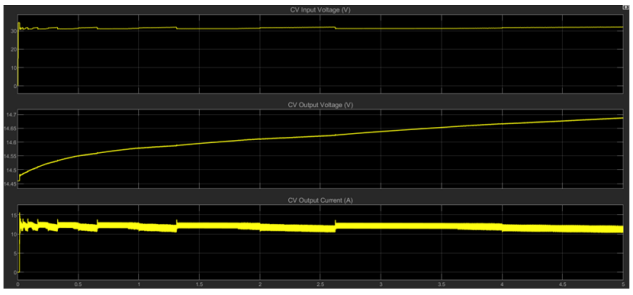

Fig. 21. (From Top to Bottom) Input voltage, output voltage and output current.

For P_o graph, we can again observe that the graph shape is similar to output current I_o, hence we can infer that the output power is mostly influenced by the output current with its irregular current changes before reaching steady state, with the output voltage only having minor influence with a small rate of increase in its voltage. The power ripple is also more

noticeable in output power compared to input power P_I due to the capacitor and inductor components influencing the output power. However, for input power there is an overshoot at the transient period before going back to steady state.

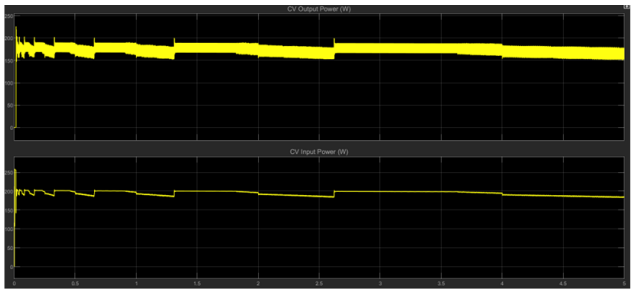

Fig. 22. (From Top to Bottom) Output power and input power.

The error values can be obtained by comparing the value calculated and the value recorded in Table 8. The output power parameter gives the highest amount of error output, while the output voltage has the smallest amount of error output. The errors happen due to resistances in components as well as imperfect parameter specification for capacitors and inductors, as well as power losses in the system happens. According to Faraday's law of induction, there will be a voltage V_L induced across the inductor where it opposes the flow of input voltage. This causes the reduction of output voltage at the battery and thus impacting the overall performance. At the same time, the inductor absorbs energy from the source and stores the energy in the form of a magnetic field.

Table 8. Simulation Result of CV Solar Battery Charger

Parameters	Simulation Results	Expected Results	% Error
Input Power, P_I (W)	185.1	213.15	-13.16
Input Voltage, V_I (V)	31.93	28	14.04
Input Current, I_I (A)	5.795	7.5	-22.73
Output Voltage, V_O (V)	14.69	15	-2.07
Output Current, I_O (A)	10.56	14	-24.57
State of charge (%)	30.02	30	0.07
Output Power, P_O (W)	155.1	210	-26.14

3.5 Hill Climbing (HC) Solar Battery Charger

The overall HC solar battery charger circuit diagram is constructed as shown in Figure 23. The component POWERGUI is set up with discrete time of 1µs to run the simulation. The simulation is run and the result is recorded and shown at Table 9. In Figure 24, we can see that the graph of input voltage reaches a steady state with an average of 30V but it has a noticeable irregular voltage ripple with different amplitudes for certain periods. For V_o graph, the battery is charging with the voltage slowly increasing at a constant rate with a tiny amount of voltage ripple being observed as well. For the inductor current, the steady state of the inductor current has a more noticeable irregular current ripple in the graph. The graphs also show a faster transient time for the graph to be at a steady state.

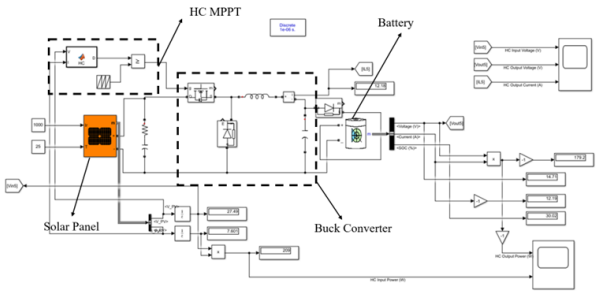

Fig. 23. Circuit design of hill climbing solar battery charger.

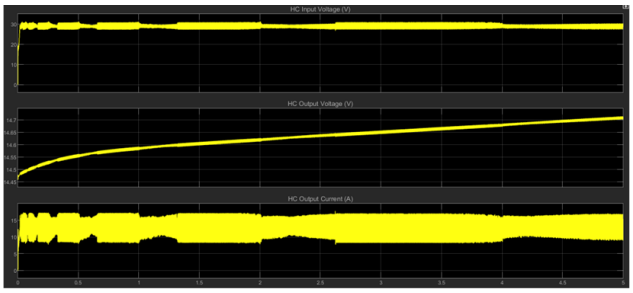

Fig. 24. (From Top to Bottom) Input voltage, output voltage and output current.

For P_o graph, we can again observe that the graph shape is similar to output current I_o with irregular voltage ripple in the graph. The power ripple is extremely noticeable in output power compared to input power P_I due to the capacitor and inductor components influencing the output power. However, for input power it is similar to input voltage graph shape instead with a gradual increase during transient period until it reaches steady state.

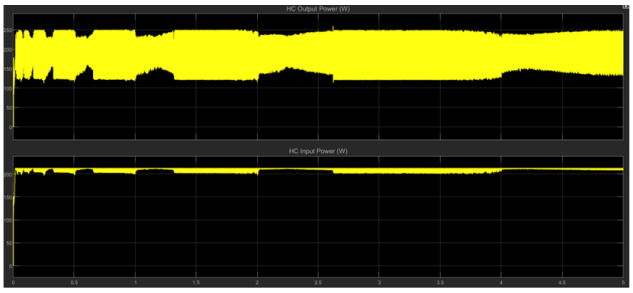

Fig. 25. (From Top to Bottom) Output power and input power.

The error values can be obtained by comparing the value calculated and the value recorded in Table 9. The output power parameter gives the highest amount of error output, while the input current has the smallest amount of error output. The errors happen due to resistances in components as well as imperfect parameter specification for capacitors and inductors, as well as power losses in the system happens. According to Faraday's law of induction, there will be a voltage V_L induced across the inductor where it opposes the flow of input voltage. This causes the reduction of output voltage at the battery and thus impacting the overall performance. At the same time, the inductor absorbs energy from the source and stores the energy in the form of a magnetic field.

Table 9. Simulation Result of HC Solar Battery Charger

Parameters	Simulation Results	Expected Results	% Error
Input Power, P_I (W)	209	213.15	-1.95
Input Voltage, V_I (V)	27.49	28	-1.82
Input Current, I_I (A)	7.601	7.5	1.35
Output Voltage, V_O (V)	14.71	15	-1.93
Output Current, I_O (A)	12.19	14	-12.93
State of charge (%)	30.02	30	0.07
Output Power, P_O (W)	179.2	210	-14.67

3.6 Performance Analysis of Various Battery Charger Circuits

The error values of voltage, current and power are placed together in a chart to compare the performance between the conventional solar battery charger and also MPPT solar battery charger. In the first chart provided in Figure 16, we can observe that the output voltage is nearly consistent across different types of circuit regardless of whether MPPT algorithms are used or not. The negative error of output voltage indicates voltage loss does happen at the output side of the circuit which is also the battery, due to the presence of other components with resistance such as diodes. The power formula (P=VI) is also required to be taken into factor, in which a loss in either current or voltage is balanced by another themselves. From the graph we can also observe that the input voltage surge occurs in CV algorithm used for solar battery charging circuit, whereas input voltage losses occurs for the rest of circuits. From the graph, we can infer that the input voltage is most stable for INC followed by HC, CV, P&O, and lastly PID. The battery load has a voltage that is constantly increasing due to its charging which contributes to instability especially when bigger load is used according to Gumilar and others (2020) [8]. Thottuvelil and Verghese (2000) said that the consequences of voltage change is the massive changes in current which overheats and reduce the battery life, due to the float charging mechanism caused by tiny impedance in the battery, hence voltage regulation is mandatory to ensure the battery is in optimal performance [9].

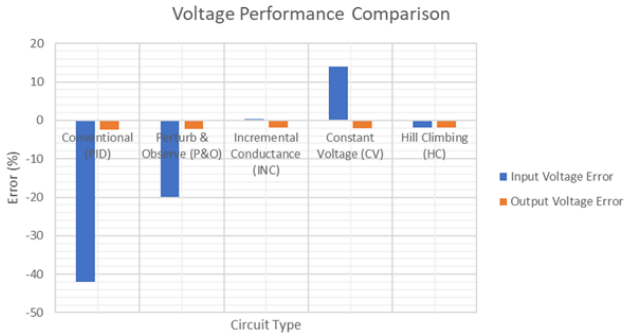

Fig. 26. Voltage performance comparison for different types of circuits.

For the second chart in Figure 27, we can observe that the output current deviation happens to be the biggest for P&O algorithm, followed by PID, CV, HC and finally INC. The loss in output current also happens due to the presence of other components with resistance such as diodes, capacitor and MOSFET which may divert some currents away into the components due to dissipation factor. The power formula (P=VI) is also required to be taken into factor, in which a loss in either current or voltage is balanced by another themselves. From the graph we can also observe that the input current surge occurs in PID, INC and HC used for solar battery charging circuit, whereas input current losses occurs for P&O and CV circuits. It is concluded that INC generally handles current stability very well, followed by HC, CV, PID and lastly P&O. The current is often impacted by switching losses which reduce battery charging efficiency, hence Hossain and Islam (2018) suggested to install some protection devices to reduce the impact, besides using MPPT [10]. Another way is to use peak current detector to maintain the stability of the inductor current which is mentioned by Dokania and others (2004) [11].

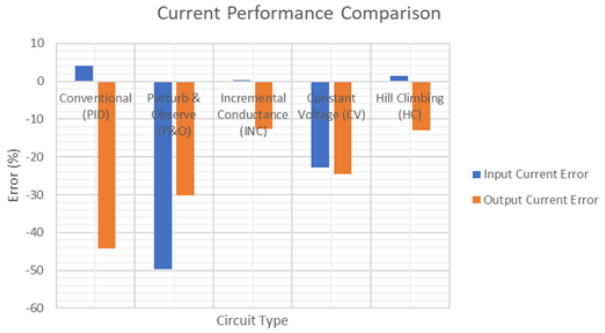

Fig. 27. Current performance comparison for different types of circuits.

For the third chart in Figure 28, we can observe that the output power losses happen to be the biggest for PID, followed by P&O, CV, HC and finally INC, which is almost similar performance as the output current losses with minor difference for PID and P&O. Thus, it can be inferred that the output current is the main factor for the changes of output power, while the input current is only corresponded to output power for P&O and CV, while other algorithms have opposite polarity. Power losses happens due to energy absorption in passive components, switching losses, diodes, and transistors, as explained by Toledo and others (2016) [12].

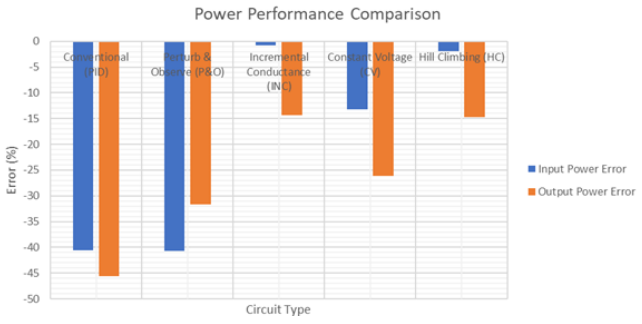

Fig. 28. Power performance comparison for different types of circuits.

Then, the performance efficiency is determined based on the input power and output power. The closer the maximum of the simulation results of the power to the expected results, the better the performance of the solar battery charging circuit. The formula below is used for both calculations of input power performance regulation and output power efficiency, and the results are tabulated in Table 10 with a graph provided in Figure 29 for comparison of regulation and efficiency.

$$\%\ Percentage = \frac{|Simulation\ Results\ (Power)|}{|Expected\ Results\ (Power)|} \times 100\% \quad (13)$$

Table 10. Power Regulation and Efficiency for Solar Battery Charger Circuits

Circuit Type	Input Power (W)	Output Power (W)	Input Power Performance Regulation	Output Power Efficiency	Remark (R&E)
PID	126.6	114.2	59.39%	54.38%	Poor & Very Low
P&O	126.5	143.5	59.35%	68.33%	Very Poor & Low
INC	211.4	180	99.18%	85.71%	Very Good & Very High
CV	185.1	155.1	86.84%	73.86%	Average
HC	209	179.2	98.05%	85.33%	Good & High

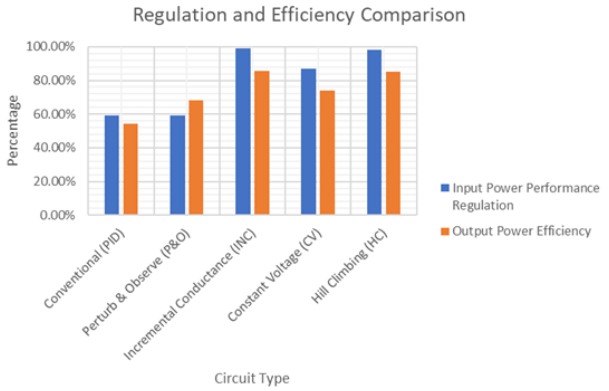

Fig. 29. Power regulation and efficiency comparison for different types of circuits.

From the above graph provided, it is found that INC algorithm provides the best overall efficiency performance for both input and output power. Theoretically, a perfect power supply will have 100% regulation and efficiency, however due to resistances in components as well as within the PV module itself, ripple voltage and current will produce, and in return, ripple power happens at both input and output which contributes to power losses according to Elkhateb and others (2015) [13]. In another research work, Schofield and others (2012) conclude that the increment of ripple current amplitude at solar cell will reduce the overall output power performance [14]. Other factor that impacts the power efficiency are duty ratio as mentioned by Naik and Samuel (2017) and harmonic distortion which is postulated by Djeghader and others (2019) [15] [16].

Next, the output power oscillation is evaluated at steady state. Oscillation frequently happens in PV which impacts inter-area oscillations negatively and causes damping according to Hasan and others (2018) [17]. The bigger the oscillation, the higher the performance losses of the battery charging system and the more unstable the output. Output power oscillation is the maximum output power subtracted with minimum output power. The maximum value is obtained at the upper peak of the output power graph in steady state while the minimum value is obtained at the lower peak of the output power graph in steady state using signal statistics in MATLAB. The order of oscillation ranging from best to worst is arranged from top row of table to bottom row in Table 11.

Table 11. Output Power Oscillation of Battery Charging Systems at Steady State

Circuit Type	Minimum Output Power (W)	Maximum Output Power (W)	Output Power Oscillation (W)	Remark
PID	114.0	114.2	0.2	Extremely stable
CV	150.7	203	52.3	Very stable
INC	146.3	229.7	83.4	Stable
HC	113.1	259.7	146.6	Unstable
P&O	-0.4	352.1	352.5	Extremely Unstable

While the results above show that MPPT are capable to regulate the oscillation, to reduce them further, Zeng and others (2016) proposes using control strategies such as increasing number of electrical energy storing devices like capacitors to ensure PV stability [18]. Examples of this strategy include hybrid usage of pulse capacitor and battery as suggested by Long and others (2015) [19].

After that, the transient time and state-of-charge relating to charging time are also evaluated in Table 12. The transient time is the time taken to reach steady state, while charging time is evaluated based on the final value of the state of charge of the battery load. The faster both the transient time and charging time, the faster the system to stabilize its performance and increase the state-of-charge of battery, which means better performance of the MPPT used for the battery charging systems. The transient time criteria is often linked to issues of degradation in PV module according to Li and others (2016), hence the performance needs to be evaluated based on transient time. [20] For the healthy performance of the battery, Chiasson and Vairamohan (2005) suggest the state-of-charge to be maintained in between 20% to 95%, which in the experiment used 30% as the parameter. [21] The time transient for P&O is unable to be determined due to extremely unstable oscillation. The order of time-response parameters ranging from best to worst is arranged from top row of table to bottom row.

Table 12. Transient Time and Battery State-of-charge for Solar Battery Charger Circuits

Circuit Type	Transient Time (s)	State-of-charge Reached at 5 Second (%)	Remark (Transient)	Remark (Charging)
CV	0.02	30.02	Extremely fast	Fast
HC	0.03	30.02	Very fast	Fast
INC	0.3	30.02	Fast	Fast
PID	3.16	30.01	Slow	Slow
P&O	Unknown	30.01	None	Slow

Thus, the performance are summarized in Table 13 with descending order from best to worst based on composite

factors with parameter priority is in descending order from left to right. Hence, the most important parameter is the output power efficiency due to our main goal is to maximize the usage of power and reduce the losses, followed by the input power regulation which is important to minimize input error and causing indirect losses into the components. Oscillation affects the overall battery charging system, and faster transient times means the system is less impacted by disturbance that affects the performance. Charging time is at the bottom priority due to most MPPT providing similar results due to the limitation of simulation for a longer time in MATLAB. Based on Table 13, it is found that INC algorithm provides the best overall efficiency performance for both input and output power, where the INC algorithm is able to utilize the most out of the solar energy through irradiance and temperature factor without having huge power losses inside the photovoltaic cell while keeping the output power efficiency at a high level to maximize the charging performance. For transient time, charging time and stability or oscillation, these variables have an adequate performance, although there are some MPPT that performs better than Incremental Conductance. In Table 13, Power Output Efficiency is shortened as Power Output E., Power Input Regulation is shortened as Power Input R., Transient Time is shortened as T. Time, and lastly Charging Time is shortened as C. Time.

Table 13. Performance Summary for Solar Battery Charger Circuits

Circuit Type	Power Output E.	Power Input R.	Oscillation or Stability	T. Time	C. Time
INC	Very High	Very Good	Stable	Fast	Fast
HC	High	Good	Unstable	Very Fast	Fast
CV	Average	Average	Very Stable	Extremely Fast	Fast
PID	Very Low	Poor	Extremely Stable	Slow	Slow
P&O	Low	Very Poor	Extremely Unstable	None	Slow

4. CONCLUSION

Here, all the results are performed for voltage controller and various MPPT algorithms for the solar battery charging system. The discussion and analysis of the performance are also completed for PID controller and various algorithms. This section summarizes the outcome of the report and provides suggestions and recommendations to improve the results further. In this project, a solar charging battery circuit using buck converter is designed and simulated to find out the performance of the design and also evaluate the best MPPT algorithm for the overall performance. The outcome of the project shows the current, voltage and power changes under different MPPT algorithms. Comparing the conventional solar battery charger system with MPPT solar battery charger system, the biggest noticeable difference is the transient period of the parameters, where the conventional system takes a longer time to stabilize the output and also having irregularities at steady state compared to other MPPT algorithms. Most MPPT algorithms are able to define the transient period clearly and also stabilize the output quickly, thus providing optimization to the system performance. Different types of MPPT algorithms will affect the outcome of voltage, current and power performance. Some MPPT algorithms, such as P&O and HC causes huge voltage and current ripple in the circuit, hence they are less suitable for performance optimization due to the fluctuation of the output that causes instability in performance. Generally, MPPT algorithms are able to provide an adequate power efficiency for input power and output power compared to conventional battery charging system without MPPT, with the INC algorithm provides the best optimization when looking at the composite outcomes together. The objective for improving the performance of battery charging system using MPPT algorithm is achieved with the results of current, voltage and power being presented showing which MPPT algorithm solves or mitigate the issues better. The difference between the performance of the conventional solar battery charging system with MPPT-based solar battery charging system are also realized based on output graphs and error comparison, with causes and effects analyzed thoroughly. For the best MPPT algorithm for the solar battery charging system, it is proven that INC achieves the best result through experimentation. However, the P&O algorithm performance is difficult to evaluate with various potential reasons such as coding and battery charging issues. More concrete method of obtaining and comparing results can be further continued by varying the irradiance and temperature for further research. The P&O algorithm can be researched further for causes of the unusual waveform result in the coding. Besides, more data of irradiance and temperature from real world can be researched and applied into the study to improve the comparison of the MPPT algorithms with real life application.

ACKNOWLEDGEMENT

The authors would like to acknowledge and thank the Faculty of Electrical and Electronic Engineering, Universiti Tun Hussein Onn Malaysia for providing support and guidance.

REFERENCES

[1] Sutedjo, Asrarul Qudsi, O., Ardianto, A., Septi Yanaratri, D., Suhariningsih, and Darwis, M., “Design and Implementation Buck Converter for 540WP Solar Charger Using Fuzzy Logic Control”, E3S Web of Conferences, 2018, vol. 43. doi:10.1051/e3sconf/2018430100

[2] C. Lapsongphon and S. Nualyai, "A Comparison of MPPT Solar Charge Controller techniques: A Case for Charging Rate of Battery," 2021 Research, Invention, and Innovation Congress: Innovation Electricals and Electronics (RI2C), 2021, pp. 278-281, doi: 10.1109/RI2C51727.2021.9559787.

[3] Podder, A.K., Roy, N.K., & Pota, H.R. (2019). MPPT methods for solar PV systems: a critical review based on tracking nature. IET Renewable Power Generation. MPPT Methods for Solar PV Systems: A Critical Review Based on Tracking Nature. IET Renewable Power Generation. 13. 10.1049/iet-rpg.2018.5946.

[4] D. Rezzak, A. Sitayeb, Y. Houam, K. Touafek and N. Boudjerda, "A New Design of Lead-Acid Battery Charger Based on Non-Inverting Buck-Boost Converter for the Photovoltaic Application," 2018 6th International Renewable and Sustainable Energy Conference (IRSEC), 2018, pp. 1-7, doi: 10.1109/IRSEC.2018.8703034.

[5] F. L. Tofoli, D. C. Pereira, W. J. Paula, "Comparative Study of Maximum Power Point Tracking Techniques for Photovoltaic Systems", International Journal of Photoenergy, vol. 2015, Article ID 812582, 10 pages, 2015. https://doi.org/10.1155/2015/812582

[6] S. M. Fatemi, M. S. Shadlu and A. Talebkhah, "Comparison of Three-Point P&O and Hill Climbing Methods for Maximum Power Point Tracking in PV Systems," 2019 10th International Power Electronics, Drive Systems and Technologies Conference (PEDSTC), 2019, pp. 764-768, doi: 10.1109/PEDSTC.2019.8697273.

[7] L. Ardhenta, M. R. Ansyari, R. K. Subroto and R. N. Hasanah, "DC Voltage Regulator using Buck-Boost Converter Based PID-Fuzzy Control," 2020 10th Electrical Power, Electronics, Communications, Controls and Informatics Seminar (EECCIS), 2020, pp. 117-121, doi: 10.1109/EECCIS49483.2020.9263425.

[8] L. Gumilar, M. Sholeh, S. Netanel Rumokoy and D. Monika, "Analysis Voltage Stability in the Interconnection of Battery Charging Station and Renewable Energy," 2020 2nd International Conference on Cybernetics and Intelligent System (ICORIS), 2020, pp. 1-6, doi: 10.1109/ICORIS50180.2020.9320761.

[9] V. J. Thottuvelil and G. C. Verghese, "Stability analysis of a digitally controlled battery plant," 2000 IEEE 31st Annual Power Electronics Specialists Conference. Conference Proceedings (Cat. No.00CH37018), 2000, pp. 1369-1374 vol.3, doi: 10.1109/PESC.2000.880508.

[10] M. K. Hossain and M. R. Islam, "Power Stage Design of a Synchronous Buck Converter for Battery Charger Application," 2018 International Conference on Advancement in Electrical and Electronic Engineering (ICAEEE), 2018, pp. 1-4, doi: 10.1109/ICAEEE.2018.864296

[11] R. K. Dokania, S. K. Baranwal and A. Patra, "Peak current detector based control of DC-DC buck converter for portable application," Proceedings of the IEEE INDICON 2004. First India Annual Conference, 2004., 2004, pp. 594-596, doi: 10.1109/INDICO.2004.1497829.

[12] D. A. Toledo Ortiz, L. G. Gonzalez, O. Carranza and R. G. Baculima, "Performance analysis of a battery charger with BQ24650," 2016 IEEE 36th Central American and Panama Convention (CONCAPAN XXXVI), 2016, pp. 1-5, doi: 10.1109/CONCAPAN.2016.7942379.

[13] A. Elkhateb, N. A. Rahim and B. W. Williams, "Impact of fill factor on input current ripple of photovoltaic system," 2015 International Conference on Renewable Energy Research and Applications (ICRERA), 2015, pp. 120-123, doi: 10.1109/ICRERA.2015.7418480.

[14] D. M. K. Schofield, M. P. Foster and D. A. Stone, "Impact of ripple current on the average output power of solar cells," 6th IET International Conference on Power Electronics, Machines and Drives (PEMD 2012), 2012, pp. 1-5, doi: 10.1049/cp.2012.0333.

[15] M. V. Naik and P. Samuel, "Effect of duty ratio on fuel cell ripple current, power losses and converter efficiency," 2017 IEEE PES Asia-Pacific Power and Energy Engineering Conference (APPEEC), 2017, pp. 1-6, doi: 10.1109/APPEEC.2017.8308960

[16] Y. Djeghader, Z. Chelli, M. Hachichi and S. Djellabi, "Investigation of Harmonics Problems in Grid Connected PV-Wind-Battery for Household Applications," 2019 1st International Conference on Sustainable Renewable Energy Systems and Applications (ICSRESA), 2019, pp. 1-6, doi: 10.1109/ICSRESA49121.2019.9182643.

[17] A. K. Hasan, M. H. Haque and S. M. Aziz, "Application of Battery Energy Storage System to Improve Damping of a Simple Power System," 2018 10th International Conference on Electrical and Computer Engineering (ICECE), 2018, pp. 117-120, doi: 10.1109/ICECE.2018.8636810.

[18] Zhirong Zeng, Hao Yi, Feng Wang, Fang Zhuo and Zhenxiong Wang, "A novel control strategy of photovoltaic-battery system for restraining the photovoltaic power fluctuations and suppressing the low frequency oscillations of power system," 2016 IEEE 8th International Power Electronics and Motion Control Conference (IPEMC-ECCE Asia), 2016, pp. 2978-2982, doi: 10.1109/IPEMC.2016.7512770.

[19] X. Long, J. Lu, X. Zhang and C. Li, "Analysis of Voltage Oscillation in Hybrid Energy Storage System," 2015 Sixth International Conference on Intelligent Systems Design and Engineering Applications (ISDEA), 2015, pp. 139-142, doi: 10.1109/ISDEA.2015.44.

[20] X. Li, Y. Li, J. E. Seem and P. Lei, "Detection of Internal Resistance Change for Photovoltaic Arrays Using Extremum-Seeking Control MPPT Signals," in IEEE Transactions on Control Systems Technology, vol. 24, no. 1, pp. 325-333, Jan. 2016, doi: 10.1109/TCST.2015.2424857.

[21] J. Chiasson and B. Vairamohan, "Estimating the state of charge of a battery," in IEEE Transactions on Control Systems Technology, vol. 13, no. 3, pp. 465-470, May 2005, doi: 10.1109/TCST.2004.839571.